



**HAL**  
open science

## Guard cell inward $K^+$ channel activity in Arabidopsis involves expression of the twin channel subunits KAT1 and KAT2

Guillaume Pilot, Benoît Lacombe, Frédéric Gaymard, Isabelle Chérel, Jossia Boucherez, Jean-Baptiste Thibaud, Herve Sentenac

### ► To cite this version:

Guillaume Pilot, Benoît Lacombe, Frédéric Gaymard, Isabelle Chérel, Jossia Boucherez, et al.. Guard cell inward  $K^+$  channel activity in Arabidopsis involves expression of the twin channel subunits KAT1 and KAT2. *Journal of Biological Chemistry*, 2001, 276 (5), pp.3215-3221. 10.1074/jbc.M007303200 . hal-02674634

**HAL Id: hal-02674634**

**<https://hal.inrae.fr/hal-02674634>**

Submitted on 31 May 2020

**HAL** is a multi-disciplinary open access archive for the deposit and dissemination of scientific research documents, whether they are published or not. The documents may come from teaching and research institutions in France or abroad, or from public or private research centers.

L'archive ouverte pluridisciplinaire **HAL**, est destinée au dépôt et à la diffusion de documents scientifiques de niveau recherche, publiés ou non, émanant des établissements d'enseignement et de recherche français ou étrangers, des laboratoires publics ou privés.

## Guard Cell Inward $K^+$ Channel Activity in *Arabidopsis* Involves Expression of the Twin Channel Subunits KAT1 and KAT2\*

Received for publication, August 11, 2000  
Published, JBC Papers in Press, October 19, 2000, DOI 10.1074/jbc.M007303200

Guillaume Pilot‡, Benoît Lacombe‡, Frédéric Gaymard, Isabelle Chérel, Jossia Boucherez, Jean-Baptiste Thibaud, and Hervé Sentenac§

From the Biochimie et Physiologie Moléculaire des Plantes, UMR 5004 Agro-M/CNRS/INRA/UM2, Place Viala, F-34060 Montpellier Cedex 1, France

**Stomatal opening, which controls gas exchanges between plants and the atmosphere, results from an increase in turgor of the two guard cells that surround the pore of the stoma. KAT1 was the only inward  $K^+$  channel shown to be expressed in *Arabidopsis* guard cells, where it was proposed to mediate a  $K^+$  influx that enables stomatal opening. We report that another *Arabidopsis*  $K^+$  channel, KAT2, is expressed in guard cells. More than KAT1, KAT2 displays functional features resembling those of native inward  $K^+$  channels in guard cells. Coexpression in *Xenopus* oocytes and two-hybrid experiments indicated that KAT1 and KAT2 can form heteromultimeric channels. The data indicate that KAT2 plays a crucial role in the stomatal opening machinery.**

The epidermis of the aerial organs of plants presents a waxy cuticle that prevents water loss, but impedes direct access of the photosynthesizing tissues to atmospheric  $CO_2$ . Pores in the epidermis, called stomata, allow atmospheric  $CO_2$  to enter the plant for photosynthesis. By providing an access to the outer atmosphere, they also allow transpiration, *i.e.* controlled diffusion of  $H_2O$  vapor from the plant into the atmosphere, which is a driving force for the ascent of crude sap from the roots to the shoots.

Regulation of the stomatal aperture allows the plant to tune and optimize uptake of  $CO_2$  and transpiration under diverse environmental conditions. Stomatal movements result from changes in turgor of the two guard cells surrounding the pore, an increase in turgor resulting in increased opening of the stomatal pore. The changes in turgor involve ion transport from and into the guard cells through  $K^+$  and anion channels. These channels are the targets of complex transduction pathways that allow the plant to regulate stomatal opening (1). In this context, the molecular identification of guard cell ion channels was an early challenge when plant channels began to be cloned. By chance, one of the first cloned plant  $K^+$  channels, KAT1 (2), was rapidly demonstrated to be endowed with functional properties compatible with a role in mediating  $K^+$  influx (3) and to be expressed in guard cells (4), opening the way to molecular approaches. By expressing a KAT1  $Cs^+$ -resistant mutant channel in transgenic *Arabidopsis*, evidence has been

obtained that this channel functions as an inward channel ( $K_{in}$  channel)<sup>1</sup> in the guard cell plasma membrane and plays a role in stomatal opening (5). Biochemical approaches have revealed that  $Ca^{2+}$ -dependent protein kinases phosphorylate the KAT1 protein (6). A homolog of the animal  $K^+$  channel regulatory  $\beta$ -subunits has been identified and shown to interact with KAT1 (7).

On the other hand, two reports (5, 8) pointed out differences in sensitivity to external pH and to the channel blocker  $Cs^+$  between the current mediated by KAT1 after heterologous expression and the current *in situ*. Two nonexclusive hypotheses can be put forward to explain these differences. First, the differences could be due to the fact that information obtained with heterologous systems gives a distorted view of the functional properties *in planta* because of, for example, lack of interactions with endogenous proteins and/or artifactual interactions with host cell proteins (9–11). The second hypothesis is that another channel is expressed in guard cells and contributes *per se* to the inward current by forming homomeric channels and/or in interaction with KAT1 by forming heteromeric channels.

We have now identified a second gene expressed in guard cells, KAT2, for which a partial cDNA had been previously cloned (12). Electrophysiological characterization of KAT2 current in *Xenopus* oocytes revealed basic properties very similar to those of the inward current in guard cells. Regarding the sensitivity to external pH and  $Cs^+$ , KAT2 is more reminiscent of the guard cell  $K_{in}$  channels than KAT1. Like their animal counterparts, plant Shaker channels are tetrameric proteins (13). Here we also bring evidence that KAT1 and KAT2 polypeptides can assemble in heterotetramers. The results provide evidence that KAT2 is a major determinant of the inward  $K^+$  current through the guard cell membrane, a fact that should stimulate research on stomatal opening mechanisms and their regulation.

### EXPERIMENTAL PROCEDURES

**KAT2 cDNA Cloning**—The 5'-region of KAT2 cDNA (see Fig. 1C; GenBank™/EBI accession number AJ288900) was determined by RACE-PCR on poly(A)<sup>+</sup> mRNA isolated from 14-day-old plantlet leaves. Amplified fragments corresponding to the 5'-end of KAT2 cDNA were cloned and sequenced. The full-length KAT2 open reading frame was then isolated by reverse transcription-PCR on poly(A)<sup>+</sup> mRNA using a primer hybridizing at the ATG codon and containing a *SpeI* site (5'-ACTAGTATGTTGAAGAGAAAGCACCTCAACAC-3') and a reverse primer hybridizing at the stop codon and containing a *NotI* site (5'-GCGCCGCTTAAGAGTTTTCATTGATGAGAATATACAAATG-3'). The amplified fragment (2.1 kilobases) was cloned at the *EcoRV* site of

\* This work was supported by European Communities BIOTECH Program Grant BIO4-CT96 and Rhône-Poulenc. The costs of publication of this article were defrayed in part by the payment of page charges. This article must therefore be hereby marked "advertisement" in accordance with 18 U.S.C. Section 1734 solely to indicate this fact.

The nucleotide sequence(s) reported in this paper has been submitted to the GenBank™/EBI Data Bank with accession number(s) AJ288900.

‡ These authors contributed equally to this work.

§ To whom correspondence should be addressed. Tel.: 33-499-612-609; Fax: 33-467-525-737; E-mail: sentenac@ensam.inra.fr.

<sup>1</sup> The abbreviations used are:  $K_{in}$  channel, inwardly rectifying  $K^+$  channel; RACE, rapid amplification of cDNA ends; PCR, polymerase chain reaction; *GUS*, *E. coli*  $\beta$ -glucuronidase gene; P domain, pore-forming domain;  $K_{HA}$  domain, domain rich in hydrophobic and acidic residues; MES, 4-morpholineethanesulfonic acid.

pBluescript and sequenced.

**Northern Blot and Reverse Transcription-PCR Experiments**—Plants were grown *in vitro* in magenta boxes as described previously (14). Total RNA extraction and Northern blotting were performed as described previously (15). Specific probes corresponding to KAT1 and KAT2 and used in Northern blot experiments were generated by PCR (cDNA fragments encoding sequences 511–587 and 524–608 of KAT1 and KAT2, respectively). Reverse transcription and PCR were performed with Superscript II (Life Technologies, Inc.) and Extra-Pol I (Eurobio), respectively, following the manufacturers' recommendations.

**Transgenic Plants and GUS Assay**—The KAT2 promoter region was isolated from genomic DNA (ecotype Columbia) by PCR walking (16) with a reverse primer introducing a unique *Nco*I site just upstream from the ATG codon (5'-CCATGGGGTTAGTTATAAATATAGTGATG-AAACTTGTG-3'). A 1.8-kilobase fragment was isolated, cloned into pBluescript, and sequenced. The construct was digested by *Bam*HI and *Nco*I and introduced into pBI320.X (from Dr. R. Derosé; this plasmid bears a unique *Nco*I site at the initiation codon of the promoterless *GUS* 3'-nopaline synthase gene), leading to a translational fusion between the KAT2 promoter region and the *GUS* coding sequence. This construct was digested by *Bam*HI and *Sac*I and introduced into the pMOG402 binary vector (from Dr. H. Hoekema). The resulting plasmid was introduced into *Agrobacterium tumefaciens* MP90 (17). *Arabidopsis thaliana* (ecotype Columbia) was transformed with agrobacteria using the floral dip method (18). Selection of T1 seedlings was performed *in vitro* on the half-strength medium described by Murashige and Skoog (19) supplemented with 1% sucrose, 0.7% agar, and 50  $\mu\text{g}\cdot\text{ml}^{-1}$  kanamycin under the following conditions: 21/18 °C day/night temperature, 16-h photoperiod, and 150 microeinsteins $\cdot\text{m}^{-2}\cdot\text{s}^{-1}$ . For GUS assay, plants were either grown *in vitro* on the same medium and under the same conditions as described above or grown in a greenhouse on attapulgite-peat compost (14). GUS histochemical staining was performed as described previously (21). Cross-sections of GUS-stained material were prepared on hydroxyethyl methacrylate (Technovit 7100, Heraeus-Kulzer GmbH, Wehrheim, Germany)-embedded tissues with an Amersham Pharmacia Biotech microtome and were counterstained in purple by periodic acid-Schiff staining.

**Expression in *Xenopus* Oocytes and Electrophysiology**—KAT1 and KAT2 cDNAs were introduced into the pCi plasmid (Promega) under the control of the cytomegalovirus promoter. The resulting plasmids, pCi-KAT1 and pCi-KAT2, were injected into *Xenopus* oocytes (purchased from Centre de Recherches de Biochimie Macromoléculaire, CNRS, Montpellier, France) using a 10–15- $\mu\text{m}$  tip diameter micropipette and a pneumatic injector (10 nl of 1  $\mu\text{g}\cdot\mu\text{l}^{-1}$  plasmid solution/oocyte). Control oocytes were injected with 10 nl of empty plasmid solution.

Whole-cell currents were recorded as described previously (21) using the two-electrode voltage-clamp technique, 3–7 days after injection, on oocytes continuously perfused with bath solution (see figure legends). Quantitative analyses of macroscopic current that yielded the gating parameters given in Table I were performed as described previously (21).

Patch-clamp experiments were performed on devitellinized oocytes as described previously (22). Voltage-pulse protocol application, data acquisition, and data analyses were performed using pClamp (Axon Instruments, Inc., Foster City, CA), Winascd (Dr. G. Droogmans, University of Leuven, Leuven, Belgium), and Sigmaplot (Jandel Scientific, Erkrath, Germany) software.

**Two-hybrid Experiments in Yeast**—Plasmid vectors pGBT9 (23) and pACTII (kindly provided by S. Elledge, Baylor College of Medicine, Houston, TX) were used for the generation of fusion proteins with the DNA-binding domain and the activator domain of Gal4, respectively. In-frame fusions were made with the C-terminal cytoplasmic regions from KAT1 and KAT2. For KAT1, a *Nco*I site was created at the end of the S6 segment coding sequence by site-directed mutagenesis (24), the GTCGTTTCATGGACT sequence from KAT1 being replaced by GTCG-TCCATGGACT. The KAT2 insert was obtained by digestion with *Bsr*I and blunt-ending with mung bean nuclease, thus allowing the polypeptide sequence to be synthesized from Arg<sup>316</sup>. Yeast cell transformations and the assay for reporter gene expression (using *o*-nitrophenyl- $\beta$ -D-galactopyranoside as substrate) were performed as described previously (23, 25).

## RESULTS

**Cloning and Sequence Analysis**—A partial KAT2 cDNA sequence has been reported (GenBank<sup>TM</sup>/EBI accession number U25694) (12). A complete KAT2 cDNA (GenBank<sup>TM</sup>/EBI acces-

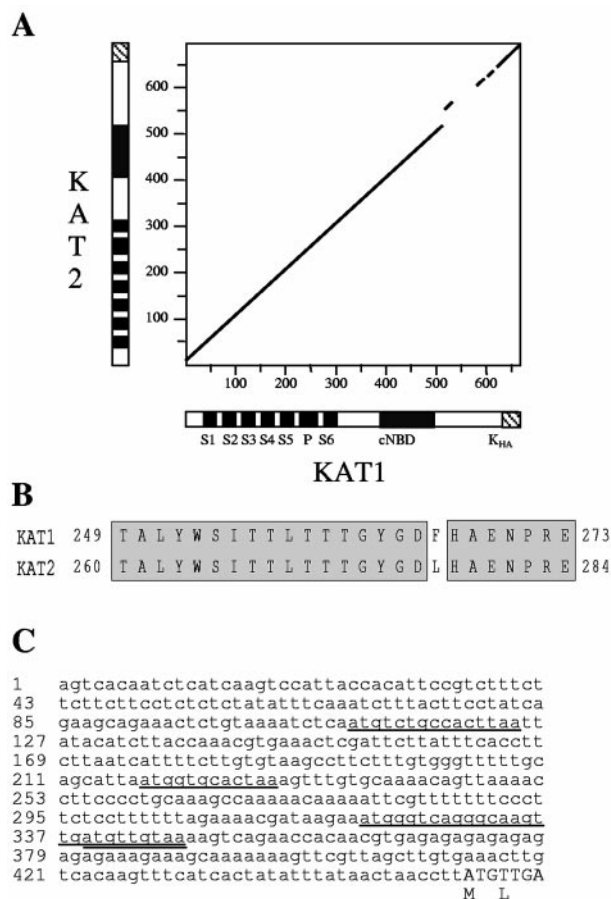


**FIG. 1. Sequence analysis.** A, dot matrix comparison (DNA Strider program, polypeptide homology matrix, stringency = 2, and window = 15 amino acids) of the deduced KAT2 amino acid sequence (GenBank<sup>TM</sup>/EBI accession number AJ288900) with that of KAT1 (GenBank<sup>TM</sup>/EBI accession number M86990). Schematic representations of the predicted channel domains are presented (bars lining the graph) on the same scale as the dot plot. S1–S6 are the six transmembrane segments forming the channel transmembrane domain. The P domain is the pore domain between S5 and S6. cNBD, putative cyclic nucleotide-binding domain. The K<sub>HA</sub> domain is the C-terminal domain thought to play a role in channel tetramerization and/or clustering in the membrane. B, alignment of the KAT1 and KAT2 pore sequences. C, sequence of the 5'-region of the KAT2 cDNA. The 5'-untranslated sequence is in lowercase letters, and the first 7 residues of the coding sequence are in uppercase letters. The four small upstream open reading frames present in the untranslated region are underlined.

sion number AJ288900) was isolated by 5'-RACE, and the promoter region was isolated by PCR walking. The sequence of a bacterial artificial chromosome containing the KAT2 gene then became available (BAC T9A21; GenBank<sup>TM</sup>/EBI accession number AL021713). Comparison of the PCR-amplified fragments (KAT2 cDNA and promoter) with that of this bacterial artificial chromosome indicated that the PCR steps had introduced no mutation.

Sequence analysis of the deduced KAT2 polypeptide identified the three domains exhibited by all plant Shaker-like channels (see "Discussion") cloned up to now (Fig. 1A): from the N to C terminus, (i) the hydrophobic core with the typical six transmembrane segments (S1–S6) and the pore-forming domain (called the P domain, between S5 and S6), (ii) the putative cyclic nucleotide-binding domain, and (iii) the so-called K<sub>HA</sub> domain, rich in hydrophobic and acidic residues and thought to play a role in channel tetramerization (13) and/or channel clustering in the membrane (26). Within the *Arabidopsis* Shaker-like family, the strongest similarities are found to KAT1. The similarities of KAT2 to KAT1 are detected all along the

polypeptide (~85% identity from the first residue to the end of the putative cyclic nucleotide-binding domain; ~65% identity in the  $K_{HA}$  domain), except in the region lying between the putative cyclic nucleotide-binding domain and the  $K_{HA}$  domain (residues 509–610 in KAT1 and residues 520–639 in KAT2) (Fig. 1A). The P domain of KAT2 differs from that of KAT1 by a single residue (Fig. 1B), and the S4 segments (with a role in voltage sensing) are identical.

Comparison of the 5'-untranslated region sequence with the sequence of the genomic clone (Fig. 1C and BAC T9A21, respectively) revealed a typical TATA box ~40 base pairs upstream from the first nucleotide of the KAT2 cDNA we have cloned, supporting the hypothesis that this cDNA could be full-length. The KAT2 5'-untranslated region is unusually long (at least 455 base pairs) compared with other *Arabidopsis* genes (27). Furthermore, it contains four ATG codons defining four small upstream open reading frames (open reading frames upstream from the main one). Such features strongly suggest a role of the transcript leader in regulation of expression (28–30).

**KAT2 Expression Pattern**—Northern blot experiments detected KAT2 mRNA in aerial organs and not in roots (Fig. 2A). Reverse transcription-PCR experiments failed to detect KAT2 transcripts in roots (data not shown), indicating that expression of KAT2 is restricted to aerial organs. Localization of expression was further investigated using transgenic plants carrying the *Escherichia coli*  $\beta$ -glucuronidase gene (*GUS*) under the control of the KAT2 promoter region (1.8 kilobases). Reporter gene activity was analyzed on the F1 and F2 progeny of 10 independent transgenic plants. GUS activity was never detected in roots. In developing leaves, GUS staining was present in all cells (Fig. 2B). In mature leaves, the activity was mainly detected in guard cells and in minor veins (Fig. 2, C and D). Mature leaf cross-sections revealed that GUS staining in minor veins was present in phloem and not in xylem parenchyma (Fig. 2E). In hypocotyls, stems (Fig. 2F), and petioles, GUS activity was present only in guard cells. In parallel experiments on transgenic *Arabidopsis* expressing *GUS* under the control of the KAT1 promoter region (stock CS3763, *Arabidopsis* Biological Resource Center), stem guard cells never displayed GUS staining (data not shown), in accordance with the lack of expression of the reporter gene in these cells (4). The data suggest that guard cells in the stem express KAT2, but not KAT1, whereas guard cells in petioles and leaves express both channels.

**Functional Characterization in *Xenopus* Oocytes**—In *Xenopus* oocytes injected with the pCi-KAT2 plasmid, hyperpolarization of the membrane beyond  $-100$  mV elicited an inward current (Fig. 3) that was not recorded in control oocytes injected with empty pCi (data not shown). The exogenous macroscopic current displayed slow activation and deactivation kinetics (Fig. 3A) with voltage-dependent time constants (Table I). No inactivation could be seen even during hyperpolarizing pulses lasting 50 s (data not shown). The steady-state current-voltage plots (Fig. 3B) show a strong inward rectification with a threshold potential of about  $-100$  mV irrespective of external  $K^+$  concentration. The reversal potential of the KAT2 current was determined at different external  $K^+$  concentrations. Following a change in the external  $K^+$  concentration from 10 to 100 mM, the reversal potential shifted by  $57 \pm 2$  mV ( $n = 5$ ), remaining close to the  $K^+$  equilibrium potential (Fig. 3B, inset), thus indicating that the inward current mediated by KAT2 was mainly carried by  $K^+$  ions. Determination of reversal potential under pseudo bi-ionic conditions (data not shown) allowed the determination of relative permeability ratios. KAT2 displays the following permeability sequence (Eisenman's series IV):  $K^+ > Rb^+ \gg Na^+ \approx Li^+$  (Table I).

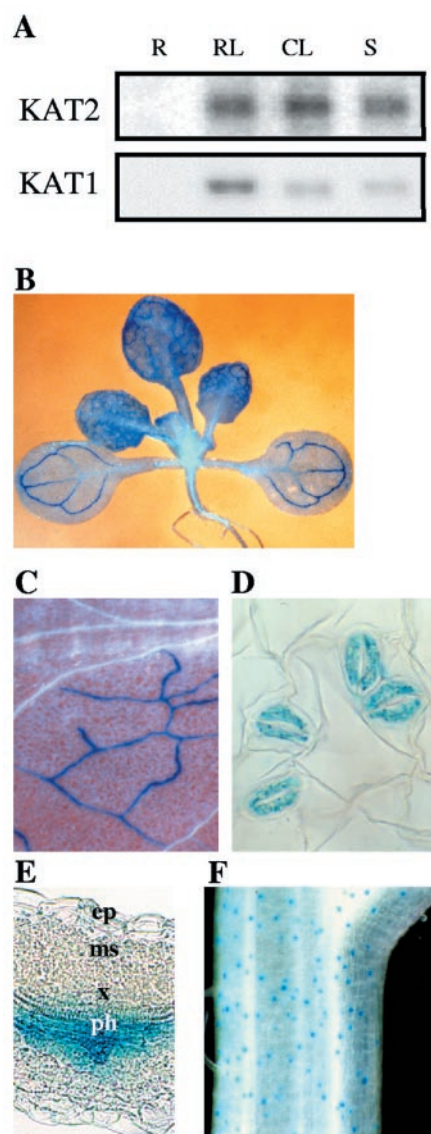
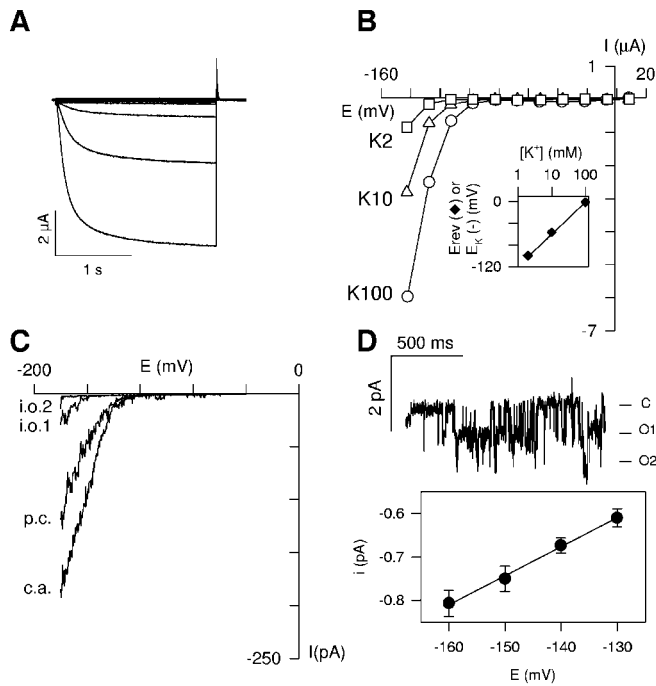


FIG. 2. **KAT2 expression pattern.** A, Northern blot analysis (5-week-old plants). Ten  $\mu$ g of total RNA extracted from roots (R), rosette leaves (RL), caulinary leaves (CL), and stem (S) were size-fractionated on an agarose gel, transferred to a nylon membrane, and hybridized with a specific probe corresponding to either KAT2 or KAT1. B–F, localization of KAT2 promoter activity in transgenic *Arabidopsis* (ecotype Columbia) using the *GUS* reporter gene. Shown are a 2-week-old seedling (B) and a rosette leaf (C), a magnification of the rosette leaf epidermis (D), a 30- $\mu$ m cross-section of a rosette leaf showing staining in the phloem (E), and the stem (F) of a 4-week-old plant. ep, epidermis; ms, mesophyll; x, xylem parenchyma; ph, phloem.

Under our experimental conditions (expression level, size of patch), macroscopic KAT2 currents mimicking whole-oocyte currents could be recorded in the cell-attached patch-clamp configuration (Fig. 3C, trace c.a.). Upon patch excision, however, the KAT2 current decreased rapidly (inside-out configuration) (Fig. 3C, traces i.o.1 and i.o.2). In this configuration, unitary currents could be resolved, which are shown in Fig. 3D. KAT2 rundown could be overcome and the initial current partly restored by cramming the patch back into the oocyte (Fig. 3C, trace p.c.). This suggested that KAT2 required intracellular factors, available in the oocyte cytoplasm, to open. From the single-channel recordings obtained in the inside-out configuration at different potentials, we were able to determine the single-channel slope conductance of KAT2: 6.7 picosiemens in symmetrical 100 mM  $K^+$  solution (Fig. 3D), a value quite similar to that reported for KAT1 (31, 32).



**FIG. 3. Functional expression of KAT2 in *Xenopus* oocytes.** *A* and *B*, two-electrode voltage clamp. The bath solution contained 1 mM  $\text{CaCl}_2$ , 1.5 mM  $\text{MgCl}_2$ , 5 mM HEPES-NaOH (pH 7.4), and 100 mM  $[\text{K} + \text{Na}]\text{Cl}$  ( $\text{K}^+$  concentration indicated below). From a holding potential of  $-40$  mV, the membrane potential was clamped (11 successive pulses of 2 s each) at values ranging from  $+10$  to  $-140$  mV in  $-15$ -mV increments. Current traces recorded in 10 mM  $\text{K}^+$  are shown in *A*. The steady-state current at the end of the activation step was plotted against membrane potential for three different external  $\text{K}^+$  concentrations: 100 mM (100K;  $\circ$ ), 10 mM (10K;  $\triangle$ ), and 2 mM (2K;  $\square$ ). The resulting current-voltage plots in *B* indicate that the potential threshold at which the current significantly increased (activation potential) was approximately  $-100$  mV. *Inset*, plotting the reversal potential ( $E_{rev}$ ) for the KAT2 current ( $\blacklozenge$ ) versus the external concentration of  $\text{K}^+$  revealed that, in this example, the reversal potential shifted by 56.5 mV for a 10-fold increase in external  $\text{K}^+$  concentration, as expected for a highly selective  $\text{K}^+$  channel. The solid line in the *inset* indicates the  $\text{K}^+$  equilibrium potential ( $E_K$ ) calculated with the Nernst equation. *C* and *D*, patch clamp. Both bath and pipette solutions contained 100 mM KCl, 2 mM  $\text{MgCl}_2$ , and 10 mM HEPES-NaOH (pH 7.4). In *C*, the current-voltage plots were elicited by 10-s potential ramps from  $-180$  to  $-40$  mV. In the cell-attached patch clamp configuration, the current-voltage curve (trace *c.a.*) is reminiscent of those obtained by two-electrode voltage clamping (shown in *B*). After patch excision (inside-out configuration), the current amplitude decreased very quickly (traces *i.o.1* and *i.o.2*; obtained 10 and 20 s after patch excision, respectively). Patch cramming into the oocyte made the current increase (trace *p.c.*). In the inside-out configuration (*D*), when few channels remained active in the patch (at least two in this example), a pulse to  $-150$  mV allowed the determination of the unitary current (0.75 pA in symmetrical 100 mM KCl). The unitary current amplitudes were obtained from gaussian fit to amplitude histograms. The single-channel current-voltage curve over the voltage range from  $-130$  to  $-160$  mV (experimental points: mean  $\pm$  S.E.,  $n = 3$ ) has been fit to a linear function, which yields a unitary conductance of 6.7 pS.

As native guard cell inwardly rectifying  $\text{K}^+$  channels are known to be stimulated upon external acidification (33, 34), we compared the sensitivity of KAT1 and KAT2 to external pH in parallel experiments carried out on oocytes from the same batch (Fig. 4). The activation potential of KAT2 was shifted positively when the pH was decreased from 7.5 to 6.0 (Fig. 4B), leading to an increase in current amplitude at a given potential. Analyses of the corresponding  $G/G_{\max}$  versus potential curves (data not shown) showed that the  $G_{\max}$  value was not changed and yielded the gating parameters (Table I). Although the apparent gating charge ( $z_g$ ) was not changed, the half-activation potential ( $E_{a50}$ ) was indeed shifted by approximately

$+15$  mV when the pH was decreased from 7.5 to 6.0. By contrast, and as previously reported (35), KAT1 gating parameters were left unchanged by the pH drop (Fig. 4A), an increase in macroscopic conductance ( $G_{\max}$ ) being responsible for the increase in current (Table I).

Block by external  $\text{Cs}^+$  is a classical feature of plant and animal  $\text{K}^+$  channels that is believed to involve the binding of  $\text{Cs}^+$  to some site within the pore. Pore penetration by  $\text{Cs}^+$  often results in some voltage dependence of the  $\text{K}^+$  channel block (36). As previously reported (9, 31), addition of 0.5 mM  $\text{Cs}^+$  to the external medium resulted in a voltage-dependent block of the KAT1 current (Table I). In parallel experiments on the same batch of oocytes, addition of  $\text{Cs}^+$  resulted in a voltage-independent block of KAT2 inward currents (Fig. 5, *A* and *B*; and Table I). The inhibition constant of this block, estimated from the data shown in Fig. 5B, is 2.5 mM. It is worth noting that the sequences of the pore domains of KAT1 and KAT2 differ by a single amino acid, Phe<sup>266</sup> in KAT1 corresponding to Leu in KAT2 (Fig. 1B). In this context, a KAT1-F266L mutant channel (a gift from R. Hedrich, University of Würzburg, Würzburg, Germany), *i.e.* a KAT1 mutant with the pore sequence of KAT2, was studied. The  $\text{Cs}^+$  sensitivity of the mutant channel is clearly voltage-dependent and reminiscent of that of KAT1 (Fig. 5C). Therefore, the pore domain sequence is not the only determinant of KAT1 and KAT2 sensitivity to  $\text{Cs}^+$ . Further pharmacological characterization revealed that KAT2 has a lower sensitivity to external  $\text{Ba}^{2+}$  than KAT1 and a sensitivity to external tetraethylammonium similar to that of KAT1 (Table I).

**Interactions with KAT1**—Single-point mutations in the KAT1 P domain have been recently reported to yield dominant-negative mutants (37). We introduced a mutation in KAT1 (W253G) that produced electrically silent channels in *Xenopus* oocytes. Coexpression of this mutant with the wild-type KAT1 channel in *Xenopus* oocytes resulted in a lower inward current than did the expression of the wild-type channel alone (Fig. 6A). Such an effect indicates that the KAT1-W253G mutant has a dominant-negative capability, *i.e.* that it can interact with the wild-type polypeptide, leading to formation of channels that are not functional or not targeted to the membrane. Interestingly, coexpression of the KAT1-W253G mutant with KAT2 decreased the inward current as well (Fig. 6A), providing evidence that the polypeptides encoded by KAT1 and KAT2 can interact and form heterotetrameric channels.

Plant  $\text{K}^+$  channels have been shown to form tetramers through interactions involving the cytoplasmic C-terminal domain (13). We therefore investigated the possibility of interactions between the C-terminal domains of KAT1 and KAT2 using the two-hybrid system in yeast (38) and obtained positive results (Fig. 6B).

Coexpression of the wild-type KAT1 and KAT2 polypeptides in oocytes resulted in an inward current that activated at a threshold potential between those of KAT1 and KAT2. We failed to find any typical feature of this current (*i.e.* a feature that would not be reminiscent of KAT1 or KAT2 properties). Interestingly, however, the current monitored in control oocytes injected with 10 ng of either KAT1 or KAT2 plasmid was significantly smaller than that monitored in oocytes coinjected with 5 ng of each plasmid, suggesting some synergy. The physiological significance of this effect cannot be assessed at the present time. However, in the animal field, similar observations due to interaction between channel subunits have been shown to play a role *in situ* in the organism (39, 40).

#### DISCUSSION

KAT1 and KAT2 belong to the Shaker-like family of  $\text{K}^+$  channels (41), of which nine members have been identified in

TABLE I  
Comparison of functional properties of KAT1 and KAT2 channels

Permeability ratios were determined from the reversal potential obtained in external solution containing 100 mM RbCl, NaCl, or LiCl, 1 mM CaCl<sub>2</sub>, 1.5 mM MgCl<sub>2</sub>, and 5 mM HEPES-NaOH (pH 7.4) as previously described (35). Kinetic parameters, gating parameters, and pharmacological features were determined in 10 mM external K<sup>+</sup> (+90 mM NaCl). The gating parameters  $z_g$  and  $E_{a50}$  were obtained as previously described (21).  $t_{1/2}$  activation is the time for half-activation.  $\tau$  deactivation is the time for half-deactivation (obtained by a single decaying exponential fit to tail currents). Each value is mean  $\pm$  S.E. ( $n$  = number of oocytes). TEA, tetraethylammonium.

	Selectivity				
	$P_{Rb}/P_K$		$P_{Na}/P_K$		
KAT1	0.35 <sup>a</sup>		0.002 <sup>a</sup>		
KAT2	0.29 $\pm$ 0.06 (4)		<0.002 (4)		
	Kinetic parameters				
	$t_{1/2}$ activation		$\tau$ deactivation		
	-175 mV	-125 mV	-10 mV	-100 mV	
	ms		ms		
KAT1	36 $\pm$ 6 (5)	97 $\pm$ 12 (5)	20 $\pm$ 2 (9)	130 $\pm$ 6 (9)	
KAT2	47 $\pm$ 5 (5)	115 $\pm$ 10 (5)	15 $\pm$ 1 (9)	96 $\pm$ 3 (9)	
	pH effect on gating				
	$Z_g$		$E_{50}$		
	pH 7.5	pH 6.0	pH 7.5	pH 6.0	
KAT1	1.6 $\pm$ 0.1 (7)	1.5 $\pm$ 0.1 (7)	-130 $\pm$ 3 mV (7)	-131 $\pm$ 3 mV (7)	
KAT2	2.5 $\pm$ 0.1 (7)	2.5 $\pm$ 0.1 (7)	-152 $\pm$ 3 mV (7)	-137 $\pm$ 3 mV (7)	
	Pharmacology (inhibition in % of control)				
	Cs (0.5 mM)		TEA (5 mM)	Ba <sup>2+</sup> (5 mM)	
	-60 mV	-120 mV		-160 mV	-120 mV
KAT1	86 $\pm$ 2 (5)	48 $\pm$ 5 (5)	60 <sup>a</sup>	84 $\pm$ 2 (5)	77 $\pm$ 5 (5)
KAT2	66 $\pm$ 8 (6)	59 $\pm$ 8 (6)	57 $\pm$ 5 (3)	44 $\pm$ 3 (4)	54 $\pm$ 2 (4)

<sup>a</sup> Ref. 35.

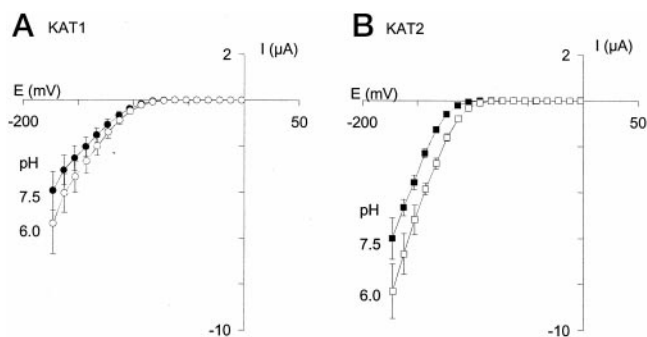


FIG. 4. Effect of external acidification on KAT1 and KAT2 macroscopic currents. Membrane currents were recorded from oocytes injected with 10 ng of either pCi-KAT2 or pCi-KAT1 using a standard staircase protocol (see Fig. 3, A and B). The external solution contained 1 mM CaCl<sub>2</sub>, 1.5 mM MgCl<sub>2</sub>, 10 mM KCl, 90 mM NaCl, and 5 mM HEPES-NaOH (pH 7.5) or 5 mM MES-NaOH (pH 6.0). A, KAT1 current-voltage relationship at pH 7.5 (●) and at pH 6.0 (○) (mean  $\pm$  S.E.,  $n$  = 4); B, KAT2 current-voltage relationship at pH 7.5 (■) and at pH 6.0 (□) (mean  $\pm$  S.E.,  $n$  = 6).

*Arabidopsis* (the whole genome having been sequenced). These channels share sequence similarities and structural homologies with animal Shaker channels (42). Shaker channels consist of four subunits arranged around a central pore (42). The core region of each subunit of the tetramer is predicted to consist of six transmembrane segments (S1–S6). S4 is characterized by the presence of several basic amino acids and forms the voltage sensor of the channel. The highest degree of sequence identity among Shaker channels is found in the so-called P domain sequence (~20 amino acids), located between S5 and S6. In the functional protein, the four P domains are assembled around the aqueous pore at the center of the structure (42).

Animal Shaker channel subunits can form heteromultimeric structures, and this process generates diversity in potassium

channel activity (43–45). Similarly, coexpression of couples of plant K<sup>+</sup> channel subunits in *Xenopus* oocytes has revealed formation of heteromultimeric structures (10, 37), providing the first support for the hypothesis that, in plants, too, functional diversity of K<sup>+</sup> channel activity could result from temporal and developmental overlapping expression patterns. However, our present knowledge of the expression pattern of the various K<sup>+</sup> channels in the plant is still very poor and mainly concerns four genes in *Arabidopsis*, namely KAT1 (4), AKT1 (20), AKT2 (46, 47), and SKOR (14), the first three of which encode K<sub>in</sub> channels and the fourth an outward channel. The available data identified KAT1 as the only K<sub>in</sub> channel expressed in guard cells (4).

KAT2 is mainly expressed in the phloem of minor veins, together with the AKT2 K<sup>+</sup> channel (46, 47), and in guard cells, together with KAT1 (4). The present data demonstrate that, in plants, too, several Shaker K<sup>+</sup> channel subunits can be expressed within a single cell type. In minor veins, KAT2 could be involved in K<sup>+</sup> loading into the phloem sap, as suggested for AKT2 (46, 47). Although this transport plays major roles, taking part in both control of phloem sap flow rate and integration of K<sup>+</sup> fluxes at the whole-plant level (48, 49), electrophysiological properties of the cell membrane in phloem tissues have never been analyzed yet because of methodological difficulties. Electrophysiological investigations have been mainly focused on guard cells for both biological (a crucial role in the control of gas exchanges between the plant and the atmosphere) and methodological (cells easily accessible to electrophysiological techniques) reasons. The discussion below concerns only K<sup>+</sup> channel activity and KAT1-KAT2 interactions in guard cells.

The functional properties of KAT2 are very similar to those reported for KAT1 (3, 31, 32, 35). Both polypeptides form voltage-gated inwardly rectifying channels, highly selective for K<sup>+</sup> and displaying the same unitary conductance (~7 picosiemens) and small differences in gating parameters (half-activation potential and gating charge). The main differences between

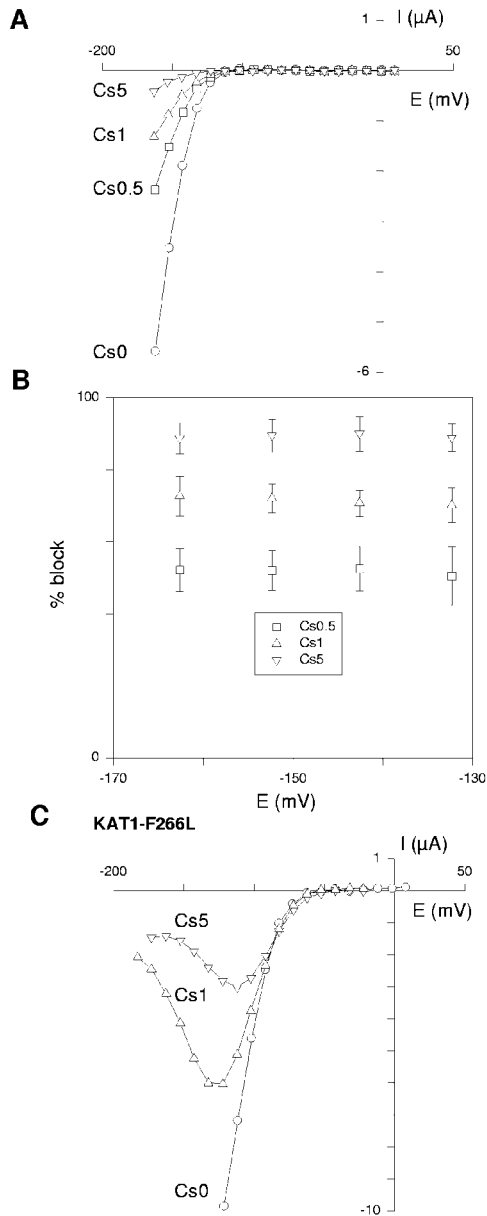


**FIG. 5. Effect of  $Cs^+$  on KAT2 currents.** Membrane currents were recorded from oocytes injected with 10 ng of pCi-KAT2 or pCi-KAT1-F266L. The external solution contained 1 mM  $CaCl_2$ , 1.5 mM  $MgCl_2$ , 5 mM HEPES-NaOH (pH 7.4), 10 mM KCl, and 90 mM  $[Na + Cs]Cl$ . **A** and **B**, sensitivity of the KAT2 current to  $Cs^+$ . Increasing  $Cs^+$  concentrations in the external medium (0 (○), 0.5 (□), 1 (△), and 5 (▽) mM) induced a decrease in the KAT2 current as shown in the current-voltage plots (**A**). This block was voltage-independent (**B**). **C**, the KAT1 mutant F266L (which corresponds to a KAT1 channel with the KAT2 pore) displays a voltage-dependent  $Cs^+$  block.

these channels detected so far concern the sensitivity to external pH and  $Cs^+$ . The sensitivity of KAT1 (expressed in *Xenopus* oocytes) to external pH has been analyzed in studies, leading to partly conflicting results. Hoshi (32) reported that acidification from pH 7.2 to 6.2 was without any effect on the current. For a larger acidification, from pH 7.4 to 4.5, Hedrich *et al.* (31, 50) reported a positive shift of the half-activation potential, but no effect on the  $G_{max}$  parameter, whereas Véry *et al.* (35) reported that acidification from pH 6.4 to 5.0 was without any effect on the gating parameters (half-activation potential and gating charge), but resulted in an increase in  $G_{max}$ . As experimental conditions in heterologous systems may vary somewhat (because of endogenous reactivity to pH), we decided to check in

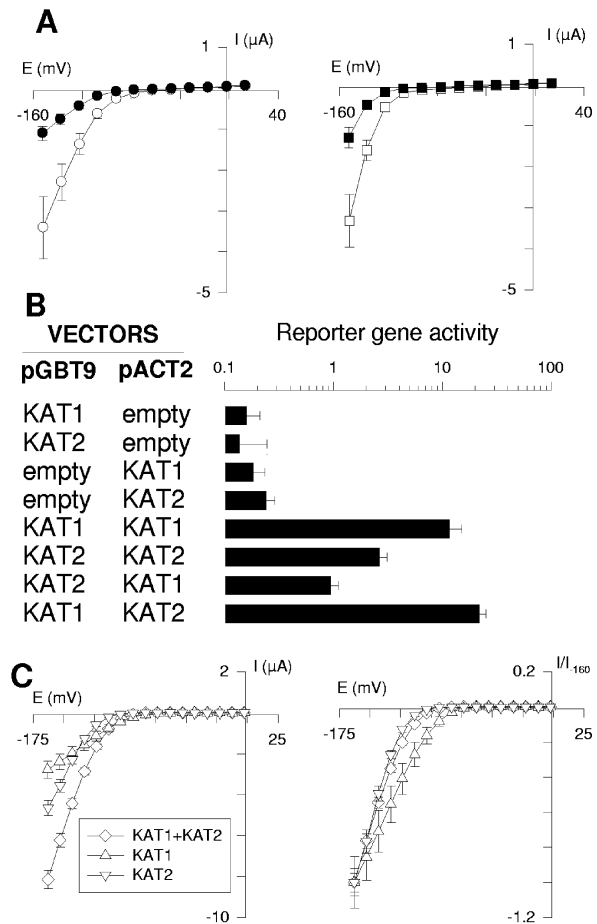


**FIG. 6. Interactions between KAT1 and KAT2.** **A**, dominant-negative experiments in *Xenopus* oocytes. KAT1 (left panel) and KAT2 (right panel) were either expressed alone (open symbols) or coexpressed with the KAT1-negative mutant KAT1-W253G (mutation W253G, not functional) in a 1:4 molar ratio (closed symbols). From a holding potential of  $-40$  mV, the membrane potential was clamped (12 successive pulses of 2 s each) at values ranging from  $+15$  to  $-150$  mV in  $-15$ -mV increments. Coexpression of KAT1 with KAT1-W253G (left panel) led to a decrease in the KAT1 current consistent with a dominant-negative effect on KAT1 expression. The same experiment with KAT2 instead of KAT1 (right panel) led to a decrease in the KAT2 current similar to the one observed for KAT1. **B**, interactions between the C-terminal domains of KAT1 and KAT2 revealed using the two-hybrid system. The pGBT9 and pACTII plasmids bearing the KAT1 or KAT2 C-terminal insert (encoding the cytoplasmic region of the channel downstream from the last transmembrane segment) or no insert (empty) were tested in the different combinations indicated.  $\beta$ -Galactosidase activities were measured following the hydrolysis of *o*-nitrophenyl- $\beta$ -D-galactopyranoside in liquid medium. The data (mean  $\pm$  S.E.,  $n = 3$ ) are given in the following units:  $1000 \times (A_{420\text{ nm}})/(reaction\ time\ in\ min)/(A_{600\text{ nm}}\ of\ the\ yeast\ culture)$ . Note the logarithmic scale. **C**, coexpression of wild-type KAT1 and KAT2 channels in *Xenopus* oocytes. Membrane currents were recorded from oocytes injected with 10 ng of pCi-KAT1 ( $\Delta$ ), 10 ng of pCi-KAT2 ( $\nabla$ ), or 5 ng of pCi-KAT1 + 5 ng of pCi-KAT2 (coexpression;  $\diamond$ ). The external solution contained 1 mM  $CaCl_2$ , 1.5 mM  $MgCl_2$ , 5 mM HEPES-NaOH (pH 7.4), 90 mM NaCl, and 10 mM KCl. From a holding potential of  $-40$  mV, the membrane potential was clamped (17 successive pulses of 2 s each) at values ranging from 0 to  $-160$  mV in  $-10$ -mV increments. **Left panel**, steady-state current-voltage relationship; **right panel**, normalized (to  $-160$  mV) current-voltage relationship (mean  $\pm$  S.E.,  $n = 4$ ).

parallel experiments, using the same batch of oocytes, whether KAT1 and KAT2 were differently affected by a moderate acidification from pH 7.5 to 6.0. The results indicate that the two channels actually display different pH sensitivities, with KAT2 being more sensitive to external acidification than KAT1. It has already been pointed out that KAT1 exhibits a weaker pH sensitivity compared with the native inward  $K^+$  channels char-

acterized in *Arabidopsis* guard cells (8). Thus, regarding the effect of external pH, KAT2 is more reminiscent of the native guard cell  $K_{in}$  channels (8, 34) than KAT1. Similarly, the  $Cs^+$  sensitivity of KAT2 is clearly closer to that of the native guard cell  $K_{in}$  channels (the block of steady-state currents by  $Cs^+$  is not voltage-dependent) (5) compared with KAT1 (voltage-dependent block) (9, 31, 51).

Guard cells respond to a number of environmental and physiological factors, including light intensity and quality,  $CO_2$  availability, humidity, plant water status, and hormones (1), with different sensitivity between abaxial and adaxial stomata (52). The differences in basic properties revealed in the heterologous context between KAT1 and KAT2 are weak and therefore unlikely to play, *per se*, crucial roles in guard cell physiology. Furthermore, the interactions that the present data reveal between KAT1 and KAT2 do not result in new current features strongly differing from those of the currents mediated by each channel expressed separately. Coexpression of these two channels is therefore not likely to provide guard cells with a mechanism generating, *per se*, diversity in channel function properties. We propose that the presence of the two genes supports channel expression control and/or generates diversity in regulatory mechanisms modulating channel function properties. In relation to this hypothesis, the length of the KAT2 leader and the presence of several upstream open reading frames strongly suggest translational regulation (28, 29). Also, the region that lies between the cyclic nucleotide monophosphate-binding domain and the  $K_{HA}$  domain in both channels displays the lowest level of sequence similarities. It could therefore be involved in specific interactions with specific regulatory proteins. Furthermore, this region bears several specific putative phosphorylation sites, present in one channel and absent from the other, which could allow specific regulation. Such diversity, together with specific expression patterns (*e.g.* leaf guard cells expressing both KAT1 and KAT2 and stem guard cells expressing only KAT2, as suggested by the present data), could allow the plant to tune, independently in each organ, the guard cell membrane  $K_{in}$  activity in relation to environmental conditions. In leaf guard cells, heteromultimerization of KAT1 and KAT2 polypeptides could further increase the diversity of the regulatory mechanisms. In conclusion, the expression of two different guard cell  $K_{in}$  channel subunits has to be taken into account in investigating stomatal opening mechanisms and their regulation.

**Acknowledgments**—We are grateful to Drs. Isabel Lefevre, Anne-Aliénor Véry, and Ingo Dreyer for critical reading of the manuscript.

#### REFERENCES

- MacRobbie, E. A. C. (1998) *Philos. Trans. R. Soc. Lond. B Biol. Sci.* **353**, 1475–1488
- Anderson, J. A., Huprikar, S. S., Kochian, L. V., Lucas, W. J., and Gaber, R. F. (1992) *Proc. Natl. Acad. Sci. U. S. A.* **89**, 3736–3740
- Schachtman, D. P., Schroeder, J. I., Lucas, W. J., Anderson, J. A., and Gaber, R. F. (1992) *Science* **258**, 1654–1658
- Nakamura, R. L., McKendree, W. L., Jr., Hirsch, R. E., Sedbrook, J. C., Gaber, R. F., and Sussman, M. R. (1995) *Plant Physiol.* **109**, 371–374
- Ichida, A. M., Pei, Z. M., Baizabal-Aguirre, V. M., Turner, K. J., and Schroeder, J. I. (1997) *Plant Cell* **9**, 1843–1857
- Li, J., Lee, Y. R., and Assmann, S. M. (1998) *Plant Physiol.* **116**, 785–795
- Tang, H., Vasconcelos, A. C., and Berkowitz, G. A. (1996) *Plant Cell* **8**, 1545–1553
- Brüggenmann, L., Dietrich, P., Dreyer, I., and Hedrich, R. (1999) *Planta* **207**, 370–376
- Véry, A. A., Bosseux, C., Gaymard, F., Sentenac, H., and Thibaud, J.-B. (1994) *Pfluegers Arch. Eur. J. Physiol.* **428**, 422–424
- Dreyer, I., Antunes, S., Hoshi, T., Müller-Röber, B., Palme, K., Pongs, O., Reintanz, G., and Hedrich, R. (1997) *Biophys. J.* **72**, 2143–2150
- Dreyer, I., Horeau, C., Lemailet, G., Zimmermann, S., Bush, D. R., Rodriguez-Navarro, A., Schachtman, D. P., Spalding, E. P., Sentenac, H., and Gaber, R. F. (1999) *J. Exp. Bot.* **50**, 1073–1087
- Butt, A. D., Blatt, M. R., and Ainsworth, C. C. (1997) *J. Plant Physiol.* **150**, 652–660
- Daram, P., Urbach, S., Gaymard, F., Sentenac, H., and Chérel, I. (1997) *EMBO J.* **16**, 3455–3463
- Gaymard, F., Pilot, G., Lacombe, B., Bouchez, D., Bruneau, D., Boucherez, J., Michaux-Ferriere, N., Thibaud, J.-B., and Sentenac, H. (1998) *Cell* **94**, 647–655
- Lobréaux, S., Massenet, O., and Briat, J. F. (1992) *Plant Mol. Biol.* **19**, 563–575
- Devic, M., Albert, S., Delseny, M., and Roscoe, T. J. (1997) *Plant Physiol. Biochem.* **35**, 331–339
- Höfgen, R., and Willmitzer, L. (1988) *Nucleic Acids Res.* **20**, 9877
- Clough, S. J., and Bent, A. F. (1998) *Plant J.* **16**, 735–743
- Murashige, T., and Skoog, F. (1962) *Physiol. Plant.* **15**, 473–497
- Lagarde, D., Basset, M., Lepetit, M., Conejero, G., Gaymard, F., Astruc, S., and Grignon, C. (1996) *Plant J.* **9**, 195–203
- Lacombe, B., and Thibaud, J.-B. (1998) *J. Membr. Biol.* **166**, 91–100
- Lacombe, B., Pilot, G., Gaymard, F., Sentenac, H., and Thibaud, J.-B. (2000) *FEBS Lett.* **466**, 351–354
- Bartel, P. L., and Fields, S. (1995) *Methods Enzymol.* **254**, 241–263
- Kunkel, T. A. (1985) *Proc. Natl. Acad. Sci. U. S. A.* **82**, 488–492
- Gietz, D., St. Jean, A., Woods, R. A., and Schiestl, R. H. (1992) *Nucleic Acids Res.* **20**, 1425
- Ehrhardt, T., Zimmermann, S., and Müller-Röber, B. (1997) *FEBS Lett.* **409**, 166–170
- Joshi, C. P. (1987) *Nucleic Acids Res.* **15**, 6643–6653
- Damiani, R. D., Jr., and Wessler, S. R. (1993) *Proc. Natl. Acad. Sci. U. S. A.* **90**, 8244–8248
- Michelet, B., Lukaszewicz, M., Dupriez, V., and Boutry, M. (1994) *Plant Cell* **6**, 1375–1389
- Lukaszewicz, M., Jerouville, B., and Boutry, M. (1998) *Plant J.* **14**, 413–423
- Hedrich, R., Moran, O., Conti, F., Busch, H., Becker, D., Gambale, F., Dreyer, I., Küch, A., Neuwinger, K., and Palme, K. (1995) *Eur. Biophys. J.* **24**, 107–115
- Hoshi, T. (1995) *J. Gen. Physiol.* **105**, 309–328
- Brüggenmann, L., Dietrich, P., Becker, D., Dreyer, I., Palme, K., and Hedrich, R. (1999) *Proc. Natl. Acad. Sci. U. S. A.* **96**, 3298–3302
- Roelfsema, M. R. G., and Prins, H. B. A. (1998) *Planta* **205**, 100–112
- Véry, A. A., Gaymard, F., Bosseux, C., Sentenac, H., and Thibaud, J.-B. (1995) *Plant J.* **7**, 321–332
- Hille, B. (1992) *Ionic Channels of Excitable Membranes*, 2nd Ed., pp. 272–302, Sinauer Associates, Inc., Sunderland, MA
- Baizabal-Aguirre, V. M., Clemens, S., Uozumi, N., and Schroeder, J. I. (1999) *J. Membr. Biol.* **167**, 119–125
- Fields, S., and Song, O. (1989) *Nature* **340**, 245–246
- Krapivinsky, G., Gordon, E. A., Wickman, K., Velimirovic, B., Krapivinsky, L., and Clapham, D. E. (1995) *Nature* **374**, 135–141
- Duprat, F., Lesage, F., Guillemare, E., Fink, M., Hugnot, J. P., Bigay, J., Lazdunski, M., Romey, G., and Barhanin, J. (1995) *Biochem. Biophys. Res. Commun.* **212**, 657–663
- Zimmermann, S., and Sentenac, H. (1999) *Curr. Opin. Plant Biol.* **2**, 477–482
- Jan, L. Y., and Jan, Y. N. (1997) *Annu. Rev. Neurosci.* **20**, 91–123
- Isacoff, E. Y., Jan, Y. N., and Jan, L. Y. (1990) *Nature* **345**, 530–534
- Ruppertsberg, J. P., Schroter, K. H., Sakmann, B., Stocker, M., Sewing, S., and Pongs, O. (1990) *Nature* **345**, 535–537
- Li, M., Jan, Y. N., and Jan, L. Y. (1992) *Science* **257**, 1225–1230
- Marten, I., Hoth, S., Deeken, R., Ache, P., Ketchum, K. A., Hoshi, T., and Hedrich, R. (1999) *Proc. Natl. Acad. Sci. U. S. A.* **96**, 7581–7586
- Lacombe, B., Pilot, G., Michard, E., Gaymard, F., Sentenac, H., and Thibaud, J.-B. (2000) *Plant Cell* **12**, 837–851
- Mengel, K., and Haeder, H. E. (1977) *Plant Physiol.* **59**, 282–284
- Lang, A. (1983) *Plant Cell Environ.* **6**, 683–689
- Hoth, S., and Hedrich, R. (1999) *J. Biol. Chem.* **274**, 11599–11603
- Ichida, A. M., and Schroeder, J. I. (1996) *J. Membr. Biol.* **151**, 53–62
- Wang, X. Q., Wu, W. H., and Assmann, S. M. (1998) *Plant Physiol.* **118**, 1421–1429